Proceedings of the 31st International Conference on Ocean, Offshore and Arctic Engineering
OMAE2012
Rio de Janeiro, Brazil · June 10-15, 2012

OMAE2012-83645

EXPERIMENTAL COMPARISON OF THREE FLOATING WIND TURBINE CONCEPTS

Andrew J. Goupee
University of Maine
Orono, Maine, USA

Bonjun Koo
Technip USA, Inc.
Houston, Texas, USA

Richard W. Kimball
Maine Maritime Academy
Castine, Maine, USA

Kostas F. Lambrakos
Technip USA, Inc.
Houston, Texas, USA

Habib J. Dagher
University of Maine
Orono, Maine, USA

ABSTRACT

Beyond many of the Earth's coasts exist a vast deepwater wind resource that can be tapped to provide substantial amounts of clean, renewable energy. However, much of this resource resides in waters deeper than 60 m where current fixed bottom wind turbine technology is no longer economically viable. As a result, many are looking to floating wind turbines as a means of harnessing this deepwater offshore wind resource. The preferred floating platform technology for this application, however, is currently up for debate.

To begin the process of assessing the relative advantages of various platform concepts for floating wind turbines, 1/50th scale model tests in a wind/wave basin were performed at MARIN (Maritime Research Institute Netherlands) of three floating wind turbine concepts. The Froude scaled tests simulated the behavior of the 126 m rotor diameter NREL (National Renewable Energy Lab) 5 MW, horizontal axis Reference Wind Turbine attached via a flexible tower in turn to three distinct platforms, these being a tension leg-platform, a spar-buoy and a semi-submersible. A large number of tests were performed ranging from simple free-decay tests to complex operating conditions with irregular sea states and dynamic winds. The high-quality wind environments, unique to these tests, were realized in the offshore basin via a novel wind machine which exhibited low swirl and turbulence intensity in the flow field. Recorded data from the floating wind turbine models include rotor torque and position, tower top and base forces and moments, mooring line tensions, six-axis platform motions and accelerations at key locations on the nacelle, tower, and platform. A comprehensive overview of the test program, including basic system identification results, is covered in an associated paper in this conference.

In this paper, the results of a comprehensive data analysis are presented which illuminate the unique coupled system behavior of the three floating wind turbines subjected to combined wind and wave environments. The relative performance of each of the three systems is discussed with an emphasis placed on global motions, flexible tower dynamics and mooring system response. The results demonstrate the unique advantages and disadvantages of each floating wind turbine platform.

INTRODUCTION

The United States has a great opportunity to harness an indigenous abundant renewable energy resource: offshore wind. In 2010, the National Renewable Energy Laboratory (NREL) estimated there to be over 4,000 GW of potential offshore wind energy found within 50 nautical miles of the US coastlines [1]. The US Energy Information Administration reported the total annual US electric energy generation in 2010 was 4,120 billion kilowatt-hours (equivalent to 470 GW) [2], slightly more than 10% of the potential offshore wind resource. In addition, deep water offshore wind is the dominant US ocean energy resource available comprising 75% of the total assessed ocean energy resource as compared to wave and tidal resources [3]. Through these assessments it is clear offshore wind can be a major contributor to US energy supplies.

The caveat to capturing offshore wind along many parts of the US coast is deep water. Nearly 60%, or 2,450 GW, of the estimated US offshore wind resource is located in water depths of 60 m or more [1]. At water depths over 60 m building fixed offshore wind turbine foundations, such as those found in Europe, is likely economically infeasible [4]. Therefore floating wind turbine technology is seen as the best option for extracting a majority of the US offshore wind energy resource.

This stated, an efficient and economical means of studying the dynamic behavior of several floating wind turbine concepts in order to advance the technology is through wind/wave basin model testing (e.g. see [5]). To date, only a few select floating wind turbine basin model tests have been performed. Principle Power Inc. tested a 1/67th scale semi-submersible wind turbine platform, WindFloat [6]. Test results were used to aid development of the first full scale WindFloat deployed in November, 2011. In 2006, Hydro Oil & Energy conducted a 1/47th scale model test of a 5 MW spar-buoy floating wind turbine at Marintek's Ocean Basin Laboratory in Trondheim, Norway [7]. Another basin test by WindSea of Norway was performed at Force Technology on a 1/64th scale tri-wind turbine semi-submersible platform [8]. These model tests provided valuable information to respective stake holders and advanced knowledge of floating wind turbine dynamics. However, these tests focused on only a single system creating difficulties with regard to comparing the relative performance of the various designs.

To address this difficulty, this paper presents a comparison of simultaneously tested floating wind turbine concepts using results of combined wind/wave 1/50th scale model testing performed at MARIN (Maritime Research Institute Netherlands) on three floating wind turbine concepts. The concepts, each supporting a model of the 5 MW, 126 m rotor diameter horizontal axis NREL Reference Wind Turbine [9], include a tension-leg platform (TLP), a spar-buoy and a semi-submersible platform. The generic platforms were modeled after proven offshore concepts and designed to provide a range of quality data for the calibration and validation of numerical floating wind turbine simulators. The test matrix, test set up and system identification of the three systems is discussed in another paper in this conference [10]. This paper presents a performance comparison of the three floating wind turbine concepts when subjected to combined dynamic wind and irregular wave environments. Quantities investigated include global motions, nacelle accelerations, tower loads and mooring loads. The results demonstrate the unique advantages and disadvantages of the three studied concepts.

MODEL DESCRIPTIONS

For the model tests, the horizontal axis wind turbine chosen for scale model construction is the NREL designed 5 MW Reference Wind Turbine [9]. The wind turbine possesses a 126 m rotor diameter and is located with a hub height of 90 m above the still water line (SWL). The flexible tower, which begins 10 m above SWL, is designed to emulate the fundamental bending frequency of the OC3 Hywind tower [11]. The wind turbine deviates from the standard NREL 5 MW Reference Wind Turbine in a few notable areas [12]. For the model wind turbine, the shaft tilt is 0°, the blade precone is 0° and the blades are rigid. The last difference is the result of two factors. First, fabricating the 17.7 mt blades at 1/50th scale requires a very light woven carbon fiber construction which is inherently stiff. Second, eliminating the added aeroelastic dynamic phenomena associated with a flexible rotor is deemed to be desirable as these effects are perceived as being beyond the scope of these tests. To mimic the first bending frequency of the OC3 Hywind tower, the tower is constructed from specifically sized aluminum tubing. Furthermore, the lower 11.3 m of the tower is of a larger diameter than the remainder of the tower in order to more closely match the OC3 Hywind tower center of gravity and fundamental bending mode shape. The total topside mass, which includes the wind turbine, tower and all accompanying instrumentation, is 699.4 mt. This value is 16.6% larger than the standard specifications for the NREL 5 MW Reference Wind Turbine and OC3 Hywind tower.

While most floating wind turbine concepts under consideration employ a horizontal axis wind turbine, the platforms employed in current concepts vary widely. Therefore, to make the test results useful to as broad an audience as possible, the previously described wind turbine and tower is tested atop three different floating platforms. The platforms, each modeled after viable offshore oil and gas platform technology, derive stability from differing mechanisms. The platforms consist of a TLP (mooring stabilized), a spar-buoy (ballast stabilized) and a semi-submersible (buoyancy stabilized). Images of the platforms employed during testing, including the wind turbine, are shown in Figure 1. Like the blades, each platform is designed to be rigid to eliminate the added complexity of a flexible platform.

Figure 1. Clockwise from left: spar-buoy, TLP and semi-submersible floating wind turbines utilized in model testing.

Each of the designs is tested in a water depth of 200 m. The first design, the TLP, is restrained by three stiff vertical tendons. The spar-buoy is moored by a spread mooring consisting of taught lines attached to the spar-buoy via a delta connection similar in nature to the type employed on the actual Statoil Hywind [11]. The last design, the semi-submersible, is

restrained by three slack catenary lines with fairlead attachments located at the top of the lower bases. Key features of the three designs are shown in Table 1 including draft,

Table 1. Select specifications for each of the platforms tested.

Platform Type	TLP	Spar	Semi
Mass w/ Turbine (mt)	1361	7980	14040
Displacement (mt)	2840	8230	14265
Draft (m)	30	120	20
CG Above Keel (m)	64.1	43.7	10.1
Mooring Spread Diameter (m)	60	890	1675
Roll Radius of Gyration (m)	52.6	53.5	31.6
Pitch Radius of Gyration (m)	52.7	53.6	32.3
Natural Surge Period (s)	39.3	43.0	107
Natural Sway Period (s)	39.3	42.8	112
Natural Heave Period (s)	1.25	28.1	17.5
Natural Roll Period (s)	3.7	32.0	26.9
Natural Pitch Period (s)	3.7	31.5	26.8
Natural Yaw Period (s)	18.2	5.5	82.3
Tower Fore-Aft Fundamental Bending Frequency (Hz)	0.28	0.43	0.35
Tower Side-Side Fundamental Bending Frequency (Hz)	0.29	0.44	0.38

displacement and mooring spread diameter. For each design, the freeboard at the tower base is 10 m. As can be seen in the table, the TLP is by far the smallest of the designs with the semi-submersible being the largest. Note, however, that these structures are generic, not optimized and are intended to exhibit the main characteristics of each concept. In addition, the TLP system does not contain any ballast unlike the other two designs. As can be seen in Table 1, the primary mass properties and motion characteristics for each of the designs, including a mounted wind turbine and tower, are also given. Examining the table, the natural periods of roll, pitch and heave motion for the moored structures indicate that the TLP system is very stiff as opposed to the spar-buoy and semi-submersible systems. In all cases, however, the natural periods of motion for these noted rigid body modes do not lie in the range of typical wave energy peak spectral periods, these being from approximately 5 to 17 seconds. Lastly, the fundamental tower bending frequencies in the fore-aft (surge) and side-side (sway) directions are also given for the three designs. It is evident from Table 1 that floating platform characteristics significantly influence the bending frequencies, with the foundations stiffer in pitch and roll exhibiting a lower bending frequency than the compliant foundations. This is not unexpected as stiffer foundations are more representative of a fixed boundary condition for the base of the tower, while the softer foundations are more akin to a free condition at the tower base (e.g. see [13]).

ENVIRONMENTAL CONDITIONS

As noted earlier, the floating wind turbine test program covers a large number of tests ranging from basic system identification to complex, coupled wind/wave tests. A description of the test matrix, as well as results for all system ID tests (static offset, hammer, free decay and response amplitude operator tests) is presented in a complementary paper [10], also previously described. With these tests already covered, this paper only presents results for the three systems subjected to combined wind and irregular wave loading. Therefore, the remainder of this section will present the details of the wind and wave environmental conditions employed throughout this paper.

The metocean conditions employed during the tests are based on measurements made from the Gulf of Maine NERACOOS floating buoy system. The wind environment during testing is created via a novel wind machine suspended above the water which produces near spatially uniform winds with a turbulence intensity at hub height of 4%. Multiple steady and dynamic winds are tested that cover a majority of the wind turbine operational wind speeds in addition to extreme, 100 year winds. However, only results using two steady winds and two temporally dynamic, NPD spectrum winds [14] are presented in the results section. The steady winds possess mean wind speeds at the 90 m hub height of U_m = 11.2 and 21.8 m/s. The NPD spectrum winds exhibit mean wind speeds of U_{10} = 17.0 and 24.0 m/s at the NPD specification height of 10 m above SWL. All winds are directed at 180 degrees and last for 3 hours. A depiction of the orientations and degrees of freedom (DOF) employed during model testing is shown in Figure 2.

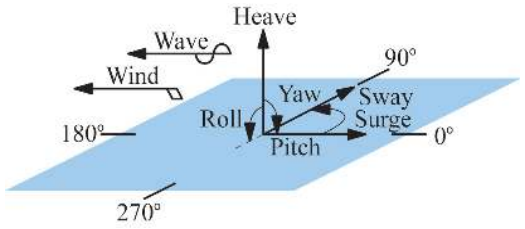

Figure 2. Orientations and degrees of freedom used during model testing.

The wind turbine operates at a rotor speed of 7.8 rpm for the U_m = 11.2 m/s condition and at a speed of 12.7 rpm for the steady U_m = 21.8 m/s and U_{10} = 17.0 m/s NPD winds. For the higher NPD wind speed, U_{10} = 24.0 m/s, the rotor is parked (0 rpm) with the blades feathered to minimize the aerodynamic drag loads. No active blade pitch control schemes are attempted and all tests utilize a fixed blade pitch setting in order to keep the number of variables that influence the global response of the floating wind turbine systems to a manageable level. For the dynamic winds, a comparison of the theoretical and obtained wind spectrums is shown in Figure 3. As can be seen in the figure, the match between the theoretical and measured spectra is quite good. The hub height statistics for the two dynamic winds are displayed in Table 2. For each of the steady and dynamic wind cases, the primary aerodynamic load contributing to global motion, thrust, varies significantly. The average thrust force for all three structures from wind only testing is found in Table 3. Note that even though the U_{10} = 24.0 m/s wind possesses the largest mean wind speed of all the winds

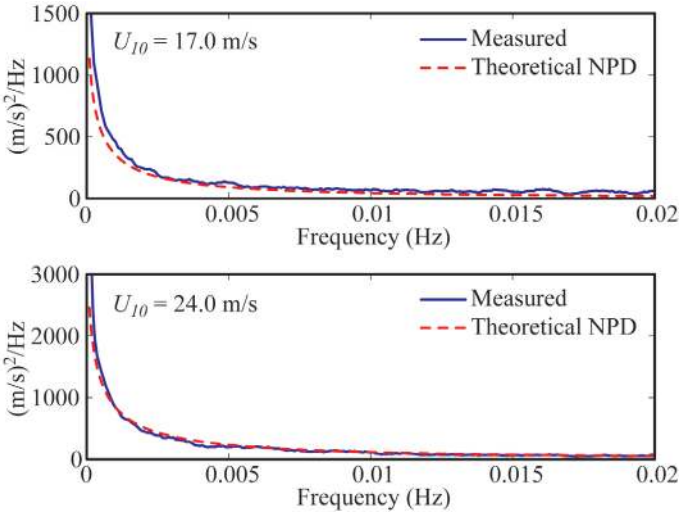

Figure 3. Theoretical and measured spectra for the U_{10} = 17.0 and 24.0 m/s NPD dynamic winds.

Table 2. Hub height (90 m) statistics for the U_{10} = 17.0 and 24.0 m/s NPD dynamic winds.

U_{10} (m/s)	Mean (m/s)	Std (m/s)	Max (m/s)	Min (m/s)
17.0	20.7	2.04	28.7	12.9
24.0	30.1	2.71	41.3	20.4

Table 3. Average thrust forces from wind only tests.

Wind Case	TLP (kN)	Spar (kN)	Semi (kN)
U_m = 11.2 m/s	263	255	203
U_m = 21.8 m/s	775	870	749
U_{10} = 17.0 m/s	642	755	683
U_{10} = 24.0 m/s	171	190	202

presented, the average thrust load is the least due to the drag reducing effect of parking the turbine rotor and feathering the blades.

Similar to the winds, multiple regular and irregular waves are tested during the model floating wind turbine experiment. However, this paper presents data from only three unidirectional irregular waves. The waves follow a JONSWAP spectrum [15] with significant wave heights of H_s = 2.0, 7.1 and 10.5 m. The peak spectral periods for these waves are T_p = 7.5, 12.1 and 14.3 s, respectively. Each of these waves is applied at 180 degrees, and thus, is aligned with the wind direction. All of these irregular waves are 3 hours in length. A comparison of the theoretical and measured spectra is shown in Figure 4. Similar to the dynamic wind results, the comparisons shown in Figure 4 show a very good agreement between the theoretical and measured spectra. The statistics for the three irregular waves, consisting of standard deviation, maximum crest height, minimum trough and maximum wave height, are shown in Table 4. As can be seen in the table, the maximum crest heights are slightly larger than the value of H_s, while the maximum wave heights are roughly double H_s for each of the waves shown.

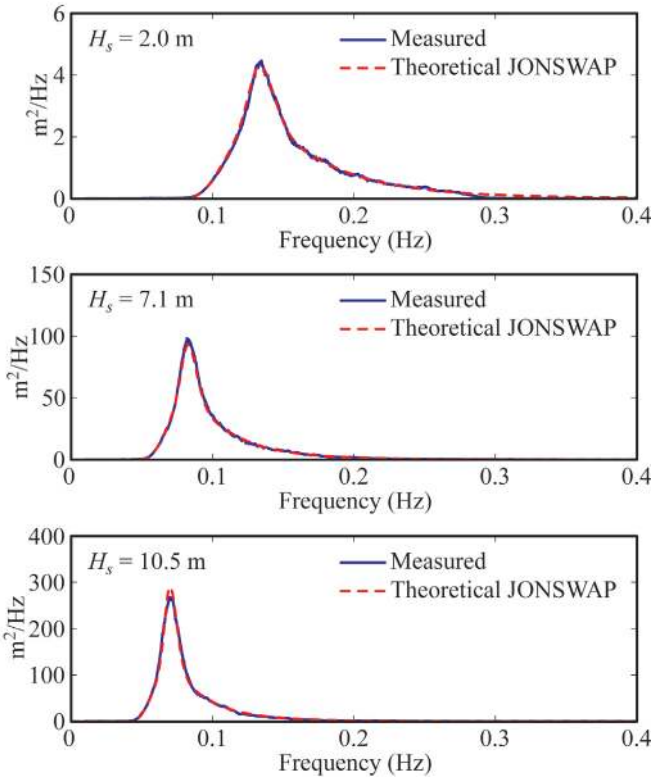

Figure 4. Theoretical and measured spectra for the H_s = 2.0, 7.1 and 10.5 m JONSWAP irregular waves.

Table 4. Statistics for the H_s = 2.0, 7.1 and 10.5 m JONSWAP irregular waves.

H_s (m)	T_p (s)	Std (m)	Max Crest (m)	Min Trough (m)	Max Wave (m)
2.0	7.5	0.49	2.14	1.87	3.64
7.1	12.1	1.79	7.20	6.37	13.58
10.5	14.3	2.62	13.59	9.58	22.01

WAVE ONLY PERFORMANCE COMPARISON

In this section, a performance comparison of the three floating wind turbine systems is presented in wave only conditions. Response spectra and statistical surge and pitch results are provided for the systems subjected to each of the three, aforementioned irregular waves to illustrate the relative motion performance of the three floating systems in irregular seas. To begin, the response spectra for the surge DOF is shown in Figure 5. The surge coordinate is reported at the structure center of gravity (CG) for all three systems, as this location provides greater physical understanding of the system translational motion. As can be seen in Figure 5, the TLP exhibits the greatest surge response in the wave energy range (0.05 to 0.15 Hz) about its CG for the three systems. The spar-buoy response is the least of the three, however, this is due in large part to the fact that the CG is very low on the structure and does not move much relative to the portion of the structure located near the waterline. The semi-submersible response is slightly less than the TLP in the wave energy range, but the

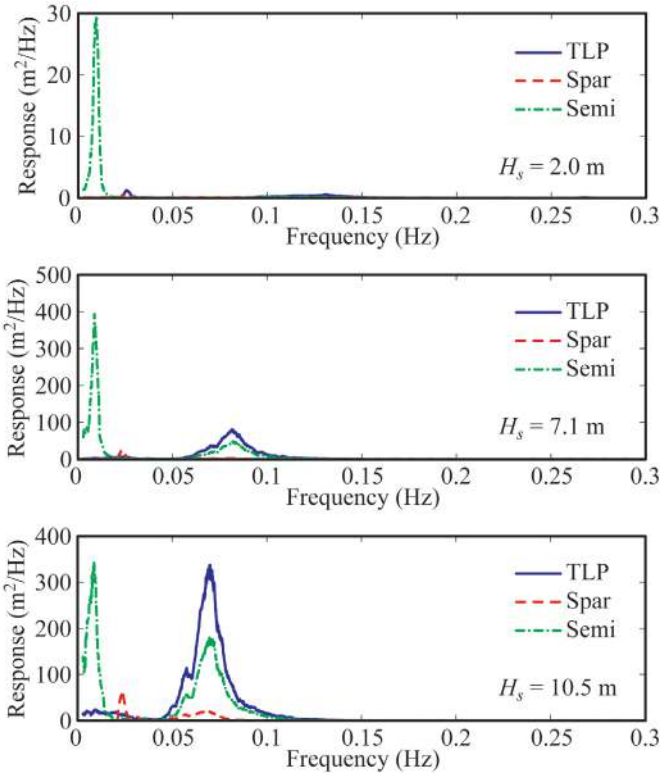

Figure 5. Surge response spectra for all three systems under wave only loading.

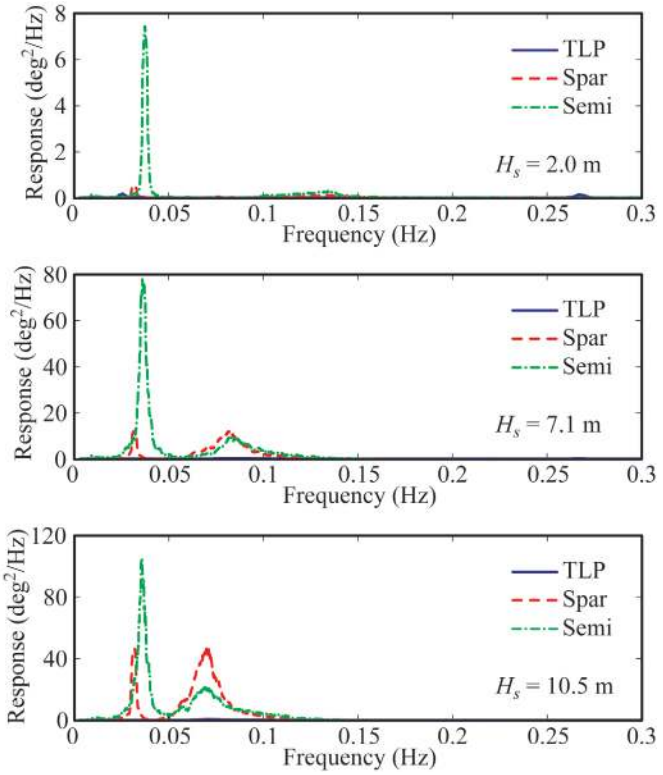

Figure 6. Pitch response spectra for all three systems under wave only loading.

semi-submersible exhibits by far the largest second-order difference-frequency associated surge motion of any of three floating turbine systems as evidenced by the significant response near the surge natural frequency of 0.009 Hz.

The second wave only comparison presented is the response spectra for the pitch motion of the structures, given in Figure 6. As one would expect, the stiff pitch restoring stiffness of the TLP is evidenced by the very low response of this system compared to the other two. Comparing the other two systems, the response is greatest for the spar-buoy in the wave energy regime, excepting the H_s = 2.0 m sea state where the semi response is slightly greater. The second-order difference-frequency response is once again greatest for the semi-submersible, with the disparity between the spar-buoy and semi-submersible being greatest as the sea state is diminished.

To complete the wave only comparison, the statistics for the surge and pitch motion are presented in Table 5. Many of the previous observations made from the frequency domain results are reinforced by the statistics of Table 5. The TLP and semi-submersible exhibit the largest minimum and maximum surge motions, with the TLP possessing the largest maximum surge for any design, 6.91 m, and the semi- submersible, the largest magnitude minimum for any of the designs, -13.72 m. Uniquely enough, the mean surge value for the TLP is quite small for all the environments, while the mean surge value for the semi-submersible grows modestly as the structure is subjected to increasing sea states. For the pitch motion, the

Table 5. Statistics for the surge and pitch motion for the TLP, spar-buoy and semi-submersible.

DOF	H_s	Mean	Std	Max	Min
TLP					
Surge (m)	2.0 m	0.07	0.21	0.86	-0.70
Pitch (deg)	2.0 m	-0.20	0.19	0.24	-0.67
Surge (m)	7.1 m	-0.11	1.37	4.49	-8.22
Pitch (deg)	7.1 m	-0.18	0.15	0.42	-0.81
Surge (m)	10.5 m	-0.33	2.53	6.91	-12.73
Pitch (deg)	10.5 m	-0.18	0.16	0.64	-1.37
Spar-buoy					
Surge (m)	2.0 m	0.18	0.21	0.97	-0.50
Pitch (deg)	2.0 m	-0.11	0.13	0.42	-0.61
Surge (m)	7.1 m	0.17	0.45	2.00	-1.87
Pitch (deg)	7.1 m	-0.12	0.57	2.13	-2.54
Surge (m)	10.5 m	0.16	0.81	3.13	-3.42
Pitch (deg)	10.5 m	-0.13	1.01	-3.65	-5.43
Semi-submersible					
Surge (m)	2.0 m	-0.73	0.38	0.70	-2.36
Pitch (deg)	2.0 m	0.05	0.24	0.97	-0.90
Surge (m)	7.1 m	-1.83	1.71	3.44	-9.68
Pitch (deg)	7.1 m	0.06	0.86	3.35	-3.92
Surge (m)	10.5 m	-2.38	2.41	5.16	-13.72
Pitch (deg)	10.5 m	0.06	1.11	4.27	-4.71

TLP motion is by far the smallest of the three, as expected. For the other two systems, the pitch response range of the semi-submersible is largest in the H_s = 7.1 m sea state, as is the pitch standard deviation. In the H_s = 10.5 m condition, the spar-buoy and semi-submersible pitch ranges are nearly identical (approximately 9 degrees) with a slightly larger pitch standard deviation for the semi-submersible as opposed to the spar-buoy.

EFFECT OF WIND ON GLOBAL PERFORMANCE

In this section, the effect of wind turbine aerodynamic loading on the global motion of the three structures is investigated. For all three structures, the response spectra and statistics of the surge and pitch DOF are investigated for three cases with an H_s = 10.5 m sea state: no wind, an operating turbine subjected to a U_{10} = 17.0 m/s wind and a parked and feathered turbine subjected to U_{10} = 24.0 m/s winds.

TLP

The response of the TLP floating wind turbine in these three conditions is investigated first. The response spectra for the surge and pitch DOF for the three cases are given in Figure 7. For both DOF, the response of the no wind and U_{10} = 24.0

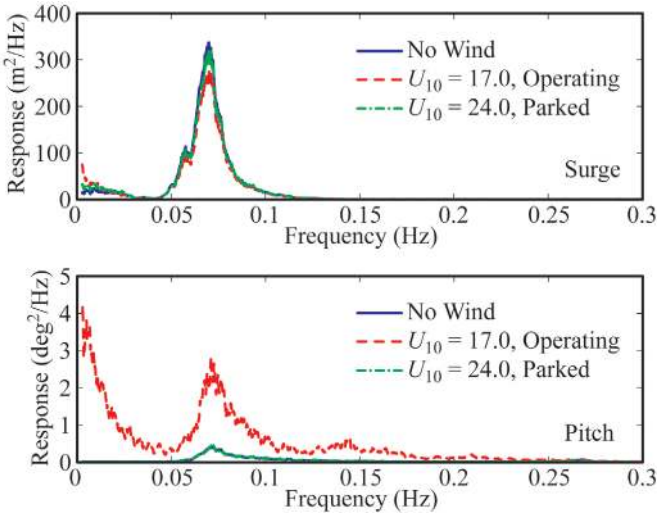

Figure 7. TLP surge and pitch response spectra for an H_s = 10.5 m sea state with three different wind conditions.

m/s cases are very similar. This indicates that even under high wind speeds, a parked and feathered rotor minimizes the impact of the wind loading on the structure's response. When the turbine is operating and the thrust loads are high in the U_{10} = 17.0 m/s case, the surge DOF exhibits increased response in the wind energy frequency range (<0.02 Hz) and is slightly damped in the wave frequency range (0.05 to 0.1 Hz). For the pitch response, the operating turbine increases the pitch response over all frequencies shown, with the greatest increases near the wind and wave energy frequencies. This is due to the fact that the TLP employed during model testing is of a small design and is not large enough to support the large overturning moment created by the thrust of the operating wind turbine in high seas, resulting in multiple slack line events. These slack line events result in infrequent, but violent pitch motions that excite a broad range of structural vibrations as evidenced by the increased pitch response shown in Figure 7. It should be noted though, that the TLP pitch response is very small, and hence, the disparity between the TLP pitch response curves in Figure 7 does not represent a great deal of energy. The statistics for the three cases are given in Table 6. For the no wind and U_{10} =

Table 6. TLP surge and pitch statistics for an H_s = 10.5 m sea state with three different wind conditions.

DOF	U_{10}	Mean	Std	Max	Min
Surge (m)	0.0 m/s	-0.33	2.53	6.91	-12.73
Pitch (deg)	0.0 m/s	-0.18	0.16	0.64	-1.37
Surge (m)	17.0 m/s	-11.03	2.46	-3.62	-22.21
Pitch (deg)	17.0 m/s	-0.52	0.41	1.48	-6.86
Surge (m)	24.0 m/s	-3.23	2.52	4.31	-15.75
Pitch (deg)	24.0 m/s	0.28	0.16	1.44	-1.72

24.0 m/s cases, the statistics are very similar, with the U_{10} = 24.0 m/s case yielding a larger magnitude mean surge and on average slightly larger magnitude extreme statistics. For the U_{10} = 17.0 m/s scenario, the mean value for surge is increased, but the standard deviation is similar to the other cases. The evidence for the slack tendon in the operating turbine case is the minimum pitch value of -6.86 degrees, this being abnormally large pitch motion for a TLP platform. If the TLP were of a sufficiently large size to prevent slack tendons, than the minimum pitch value for the U_{10} = 17.0 m/s scenario would likely decrease in magnitude by a significant amount.

Spar-buoy

Next, the results for the spar-buoy floating wind turbine are discussed. The response spectra for the surge and pitch DOF are displayed in Figure 8. For both surge and pitch DOF, the no wind and parked wind turbine cases are quite similar. As seen in Figure 8, the operating turbine increases only the second-

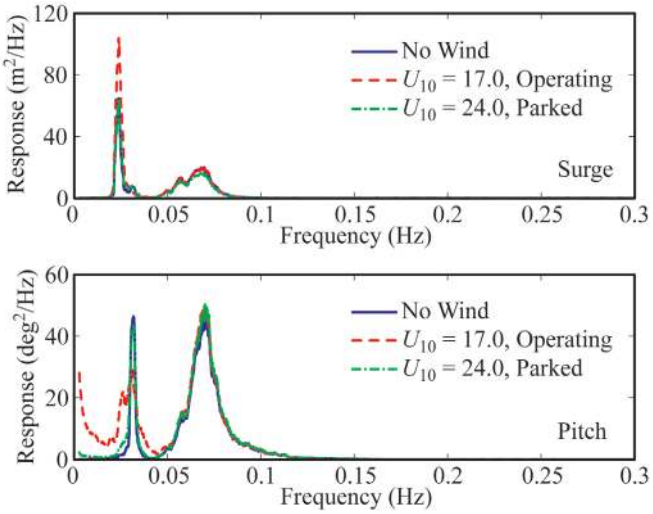

Figure 8. Spar-buoy surge and pitch response spectra for an H_s = 10.5 m sea state with three different wind conditions.

order difference-frequency surge response of the spar-buoy, this being near the spar surge natural frequency of 0.023 Hz. The pitch response, however, is increased significantly in the wind energy frequency range, with the sole exception being some damping of the pitch second-order difference-frequency response, near 0.032 Hz. The spar-buoy statistics for the two DOF for all three environments are given in Table 7. The

Table 7. Spar-buoy surge and pitch statistics for an H_s = 10.5 m sea state with three different wind conditions.

DOF	U_{10}	Mean	Std	Max	Min
Surge (m)	0.0 m/s	0.16	0.81	3.13	-3.42
Pitch (deg)	0.0 m/s	-0.13	1.01	3.65	-5.43
Surge (m)	17.0 m/s	0.14	0.92	11.23	-4.41
Pitch (deg)	17.0 m/s	-4.36	1.25	0.04	-15.26
Surge (m)	24.0 m/s	-0.08	0.76	2.93	-3.48
Pitch (deg)	24.0 m/s	-1.25	1.07	2.39	-6.13

statistics for the surge DOF for all three conditions are very similar with the lone exception being a larger range of motion for the U_{10} = 17.0 m/s case than the other two conditions. For the pitch motion, the mean value is much larger for the operating turbine than the no wind and parked turbine cases, as expected. The range of motion is also increased, however, the standard deviation is only 17% larger than the parked and feathered rotor subjected to U_{10} = 24.0 m/s winds.

Semi-submersible

Finally, the surge and pitch response spectra for the semi-submersible floating wind turbine are presented in Figure 9.

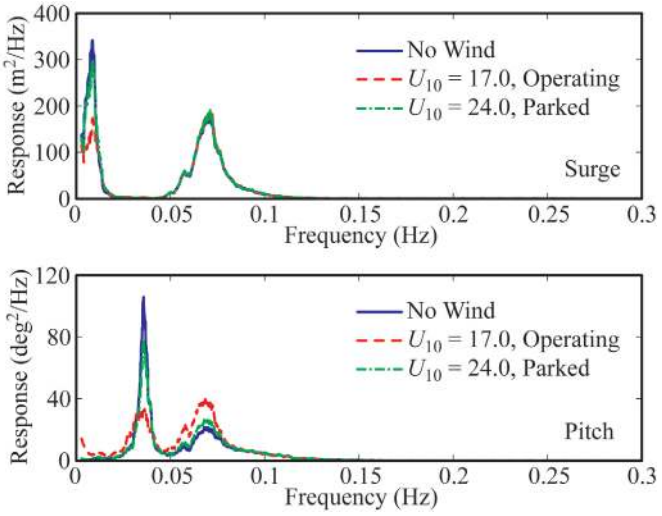

Figure 9. Semi-submersible surge and pitch response spectra for an H_s = 10.5 m sea with three different wind conditions.

Observing the figure, the parked wind turbine under U_{10} = 24.0 m/s winds provides marginal damping of the second-order difference-frequency response (0.009 Hz surge, 0.037 Hz pitch), and marginal excitation of the wave energy frequency response for pitch motion. The operating wind turbine case significantly damps the second-order response in surge and pitch, but noticeably amplifies the response in the wind and wave energy frequency ranges for pitch motion. The statistics for the cases shown in Figure 9 are given in Table 8. Similar to

Table 8. Semi-submersible surge and pitch statistics for an H_s = 10.5 m sea state with three different wind conditions.

DOF	U_{10}	Mean	Std	Max	Min
Surge (m)	0.0 m/s	-2.38	2.41	5.16	-16.72
Pitch (deg)	0.0 m/s	0.06	1.11	4.27	-4.71
Surge (m)	17.0 m/s	-9.28	2.30	-2.31	-22.28
Pitch (deg)	17.0 m/s	-3.48	1.25	1.55	-8.91
Surge (m)	24.0 m/s	-4.61	2.41	2.99	-17.78
Pitch (deg)	24.0 m/s	-0.69	1.12	3.73	-5.69

the other two floating wind turbine systems, the statistics are very similar for the no wind and parked turbine cases. The operating turbine case exhibits the largest magnitude mean pitch and surge values in Table 8, but the ranges of motion for both DOF are quite similar to the no wind and parked rotor cases.

NACELLE ACCELERATION

In this section, a study of the relative performance of the three floating wind turbine systems as measured by the nacelle surge acceleration is presented. The nacelle acceleration, which is a function of platform motion and flexible tower dynamics, is of great interest as it is indicative of the inertial loading that the wind turbine gearbox, bearings, and other complex parts will experience. For the comparison, the nacelle surge acceleration measured at 88.25 m above SWL is investigated for all three floating wind turbine systems under three distinct environmental conditions. The environmental conditions consist of H_s = 2.0, 7.1 and 10.5 m irregular sea states, each with an operating wind turbine. The H_s = 2.0, 7.1 m sea states are subjected to steady U_m = 11.2 m/s winds while the H_s = 10.5 m sea state case is subjected to U_m = 21.8 m/s steady winds. The response spectra for all three systems in each of the three conditions are displayed in Figure 10. There are several noteworthy observations to be made from the results shown in Figure 10. First, for the modest, H_s = 2.0 m sea state environment, the performance of the three systems is very similar in the wave energy frequency range (0.1 to 0.2 Hz). However, the TLP exhibits significant response at frequencies larger than the wave energy, which the other two systems do not. This energy is associated with the TLP coupled platform pitch/tower bending frequency of 0.28 Hz which is excited by the second-order sum-frequency wave loading from the small, T_p = 7.5 s sea state. While the response of all three systems is quite low in energy for the H_s = 2.0 m sea state, the prevalence of these mild sea environments indicates that this TLP may be prone to greater wind turbine and tower fatigue issues than the other systems.

Moving to the intermediate sea state of H_s = 7.1 m, the figure shows that the performance of the three systems are quite distinct. The spar-buoy system possesses the maximum peak response of the three systems with a peak that is nearly double that of the second most excited system, the TLP. While the TLP

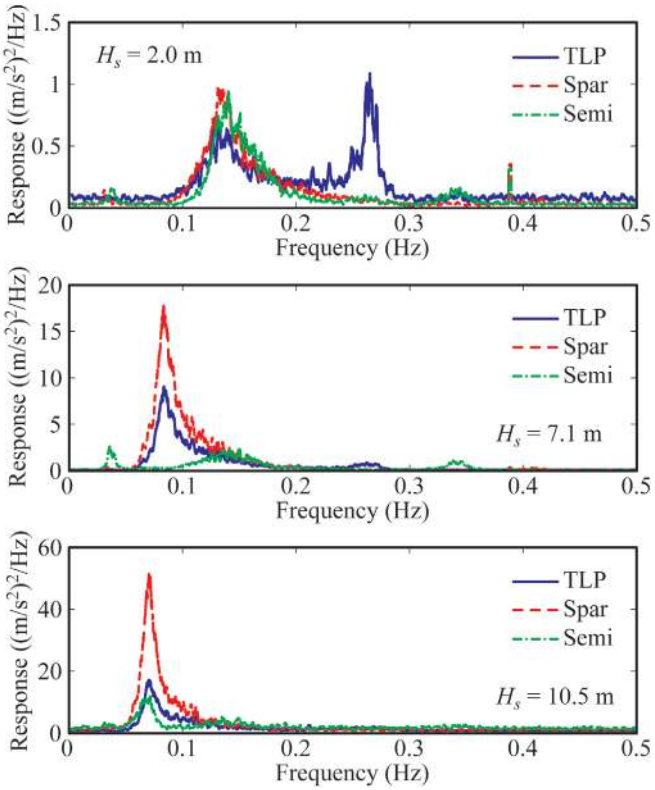

Figure 10. Nacelle surge acceleration spectra for all three systems under three distinct environmental conditions.

motion is primarily pure surge translation, the spar pivots about a point located low on the spar, near the CG, translating modest wave induced motions at the water line into large translational motions at the nacelle location. The result is the large nacelle surge accelerations seen in Figure 10 for this environmental condition. Surprisingly for this environment, the semi-submersible system nacelle surge acceleration response is greatly diminished to negligible levels over most of the wave energy range (0.05 Hz to 0.2 Hz). This is unexpected as the platform motion is substantial for this sea state with motion similar to the responses given in Figures 5 and 6. The low surge acceleration at the nacelle location is a result of the unique interplay of the surge and pitch motion characteristics for this semi-submersible in the H_s = 7.1 m environment.

The nacelle surge acceleration response comparison for the most severe environment in Figure 10, H_s = 10.5 m, shows that the response of the semi-submersible is once again the smallest, albeit only slightly less than the TLP floating wind turbine system. The spar-buoy floating wind turbine exhibits the largest response of the three, with a peak response in the frequency domain of approximately three times the TLP and semi-submersible. The reasons for the large response are similar to those identified for the H_s = 7.1 m condition, only magnified.

SYSTEM LOADS COMPARISON

In this section, a comparison of a few of the floating wind turbine system loads is presented. First, the tower base bending moment about the sway axis (pitch DOF) is presented for two different environments. This bending moment is the largest moment induced in the tower and is major design driver in the sizing of the tower. The second comparison involves the mooring line tensions for each of the designs subjected to the same wind and wave loading. These loads will indicate the relative demands of the floating wind turbine systems on the mooring and anchoring systems.

Tower Loads

For the comparison of the tower base bending moment, two environments are considered, both with an operating wind turbine subjected to a U_{10} = 17.0 m/s dynamic wind. The first possesses an H_s = 2.0 m irregular sea while the second consists of an H_s = 10.5 m sea state. The response spectra for the two conditions are shown in Figure 11. For the low energy sea state,

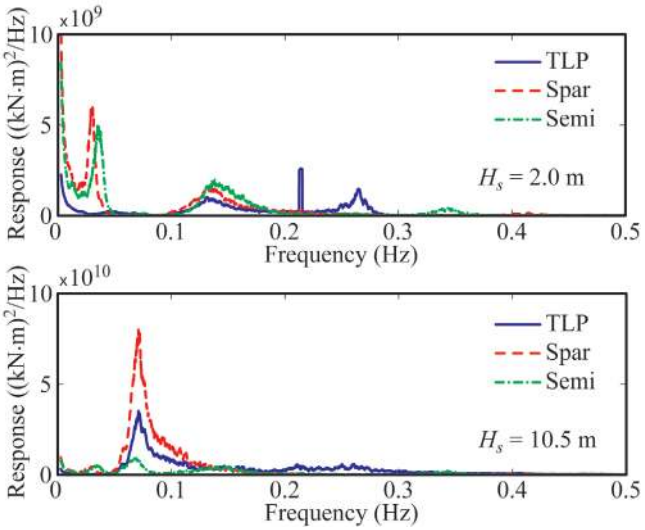

Figure 11. Tower base bending moment spectra for all three systems for two combined wind/wave loading conditions.

all three systems exhibit a moderate response in the wave energy frequency regime (0.1 to 0.2 Hz), with the semi possessing the greatest response and the TLP the least. The largest discrepancy in the three systems is the response in the frequency ranges above and below the wave energy frequency range. For low frequencies in the wind energy regime, the TLP exhibits very little response, unlike the spar-buoy and semi-submersible. The wind loading excites the rigid body pitching motion of these two systems which in turn induces significant moments at the base of the tower as a result of supporting the large nacelle and rotor weight on a tilted tower. As can be seen in Figure 11, the response at the spar-buoy and semi-submersible natural pitch frequencies (0.032 And 0.037 Hz, respectively) is quite prominent as a result of this phenomenon. At frequencies above the wave energy range, the TLP shows by far the greatest response. The response, located near the coupled platform pitch/tower bending frequency of 0.28 Hz, is excited primarily by the second-order sum-frequency wave loading of the TLP platform. The spar-buoy and semi-

submersible also exhibit some tower base bending energy at their respective tower bending frequencies of 0.43 and 0.35 Hz, albeit, at a much reduced level as compared to the TLP. A final note for this condition is that the stiff TLP system allows transmission of the turbine's once per revolutions excitation at 12.7 rpm (0.21 Hz) all the way down the tower, as evidenced by the strong peak in the signal at this frequency. Moving to the environment with the larger H_s = 10.5 m sea state, it is evident from Figure 11 that the majority of the response for all three systems is in the wave energy frequency range (0.05 to 0.1 Hz). The spar-buoy possesses the most energy in the tower base bending, with the semi-submersible the least. Since the inertial forces created by motion of the nacelle and rotor contribute greatly to the tower base moment, it is not surprising that the response trends for this sea state are similar to the Figure 10 trends for the nacelle surge acceleration in the H_s = 10.5 sea.

To complete the moment comparison, the statistics for the two conditions for all three systems are shown in Table 9. It

Table 9. Tower base bending moment statistics for all three systems for two combined wind/wave loading conditions.

H_s	Mean (kN)	Std (kN)	Max (kn)	Min (kN)
TLP				
2.0	-73,922	10,731	-23,047	-121,784
10.5	-74,291	38,757	356,510	-301,933
Spar-buoy				
2.0	-87,468	15,990	-27,787	-156,258
10.5	-79,064	45,332	91,815	-301,657
Semi-submersible				
2.0	-86,929	15,804	-28,538	-161,873
10.5	-84,358	24,572	53,555	-221,031

should be noted that the extreme minimum and maximum values for the TLP system in the H_s = 10.5 m condition are the result of tendon snapping events which cause violent pitch motions of the TLP floating wind turbine. For a properly sized (i.e., larger) TLP platform, the extreme values for the TLP system in large seas would be significantly smaller, likely less than the spar-buoy and semi-submersible. This stated, the TLP has the smallest magnitude mean, standard deviation, minimum and maximum for the H_s = 2.0 m condition. While more severe, the moment statistics for the other two systems are very similar in the smaller energy environment. For the larger sea state, the TLP appears to be the poorest performer, again, as a result of the slack tendon events encountered during testing for this TLP design. For the other two systems, the spar-buoy has a moderately larger magnitude standard deviation, minimum and maximum bending moment due mostly to the larger variations in pitch angle of the structure as displayed in Tables 6, 7 and 8.

Mooring Loads

To complete the loads comparison, the fairlead mooring line tensions for the three designs is investigated next. Note that for the spar-buoy system, only the main mooring lines are shown and the lines comprising the delta connection are omitted here. The environment investigated consists of U_{10} = 17.0 m/s winds and H_s = 2.0 m seas. The response spectra for the three mooring lines per design, denoted by orientation in degrees, are shown in Figure 12. From the figure, it is clear to see that the

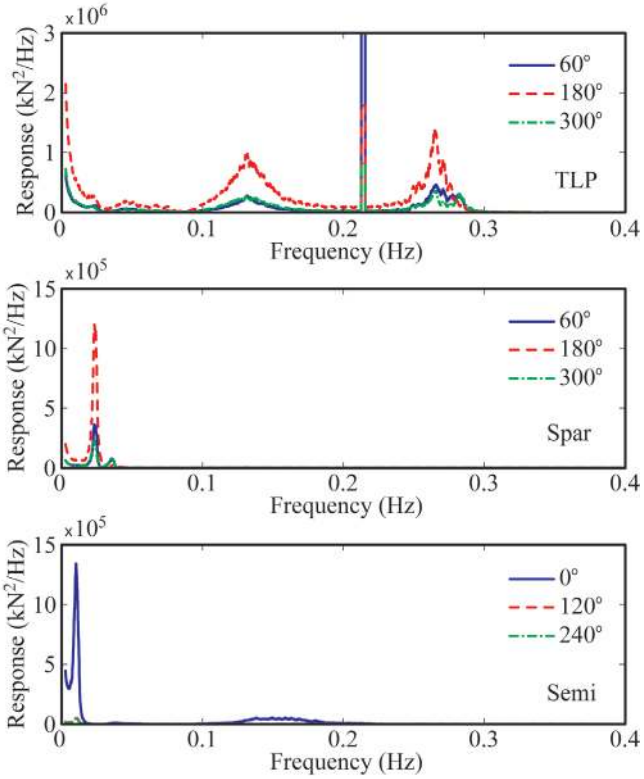

Figure 12. Fairlead mooring tension response spectra for all three systems in a combined wind and wave environment.

energy in the response of the TLP tendons is an order of magnitude greater than the response for the other two systems. This is not entirely unexpected as the TLP system gains its stability from highly loaded, stiff mooring tendons. For the spar-buoy, the mooring load response is tied closely to the surge natural period, as is the peak response of the semi-submersible. The TLP, on the other hand, exhibits significant response at frequencies associated with the wind energy, wave energy, and platform pitch/tower bending natural frequency. Surprisingly, all three TLP tendons also display a sharp response at the once per revolution rotor excitation frequency of 12.7 rpm (0.21 Hz). This is likely a result of the vertically stiff and lightweight nature of the floating TLP wind turbine system tested here.

CONCLUSIONS

This paper presented experimental performance results from wind/wave basin model testing of three floating wind turbine concepts. The three platform concepts, each supporting the same horizontal axis NREL 5 MW Reference Wind Turbine, consisted of a TLP, a spar-buoy and a semi-submersible. Results were presented for a number of wind and wave environments with an emphasis on global motions, wind excitation and damping effects, nacelle acceleration and system

tower and mooring loads. It should be noted that the following conclusions are specific to the load cases evaluated in this paper, as well as to the specific designs tested. As such, the conclusions herein are not intended to be generalized to other TLP, spar-buoy and semi-submersible designs, nor to their response under load cases not considered herein.

Wave Only Performance

The results of the wave only cases indicate that the spar-buoy tested possesses the smallest surge response in irregular seas, while the TLP system tested exhibits the smallest pitch response of any of the systems. The semi-submersible response for both DOF studied is typically in between that of the TLP and spar-buoy in the wave energy frequency range, however, the semi-submersible exhibits by far the greatest second-order difference-frequency associated motion response.

Effect of Wind Global Motions

Regarding the effect of wind, the difference in response for all three systems without wind or with a parked rotor with feathered blades in a severe dynamic wind is very similar. This indicates that feathering the rotor blades is an effective means of minimizing the impact of wind loads on the system. Unlike the feathered case, an operating wind turbine in moderate winds modifies the global motion response of the floating wind turbine. For a TLP floating wind turbine, the wind loading significantly increases the pitch response of the system, however, the pitch response energy as a whole is still quite small. For the spar-buoy and semi-submersible designs, the operating wind turbine significantly damps the second-order difference-frequency pitch response of the structures, and in the case of the semi-submersible, also damps the second-order surge response.

Nacelle Acceleration

The nacelle surge acceleration for the TLP at low energy sea states possesses significant response near the coupled platform pitch/tower bending frequency, whereas the other two systems do not. For intermediate sea states, the unique motion characteristics of the semi-submersible platform yield a near net zero motion of the 90 m hub height wind turbine, minimizing nacelle motion and the accompanying inertial loads.

Tower and Mooring Loads

The tower base bending moment for all three systems at low sea states is characterized by significant response at the platform pitch frequencies, this being above the wave energy frequency for the TLP and below it for the spar-buoy and semi-submersible. For severe sea state conditions, the tower bending moment response for all three systems is dominated by the wave and not the platform pitch frequencies. On the topic of moorings, the TLP mooring load response in the frequency domain is approximately an order of magnitude greater than for the spar-buoy and semi-submersible floating wind turbine designs. In addition, the spar-buoy and semi-submersible response is primarily located at the system surge natural frequencies whereas the TLP mooring load response is substantial in the wind energy, wave energy and coupled platform pitch/tower bending natural frequencies.

ACKNOWLEDGMENTS

The financial support from the Department of Energy through DeepCwind Grants DE-EE0002981 and DE-EE0003728, the National Science Foundation through Grant IIP-0917974 and the University of Maine is gratefully acknowledged by the authors. In addition, the expertise and support of MARIN is greatly appreciated.

REFERENCES

[1] Musial W., Ram B., 2010, *Large-Scale Offshore Wind Power in the United States*, Technical Report NREL/TP-500-40745.

[2] US Energy Information Administration, 2011, *Annual Energy Review 2010*, Technical Report DOE/EIA-0384(2010).

[3] Musial W., 2008, *Status of Wave and Tidal Power Technologies for the United States*, Technical Report NREL/TP-500-43240.

[4] Musial W., Butterfield S., Ram B., 2006, Energy from Offshore Wind, *Offshore Technology Conference*, Houston, Texas.

[5] Chakrabarti S.K., 1994, *Offshore Structure Modeling*, World Scientific Publishing Co. Pte. Ltd., Singapore.

[6] Roddier D., Cermelli C., Aubault A., Weinstin A., 2010, WindFloat: A floating foundation for offshore wind turbines, *Journal of Renewable and Sustainable Energy* 2 033104.

[7] Skaare B., Hanson T.D., Nielsen F.G., Yttervik R., Hansen A.M., Thomsen K., Larsen T.J., 2007, Integrated Dynamic Analysis of Floating Offshore Wind Turbines, *European Wind Energy Conference*, Milan, Italy.

[8] http://www.windsea.no/, accessed January 2012.

[9] Jonkman J.M., Butterfield S., Musial W., Scott G., 2009, *Definition of a 5-MW Reference Wind Turbine for Offshore System Development*, Technical Report NREL/TP-500-38060.

[10] Koo B., Goupee A.J., Lambrakos K.F., Kimball R.W., 2012, Model tests for a floating wind turbine on three different floaters, *Proceedings of OMAE 2012*, Rio de Janeiro, Brazil.

[11] Jonkman J.M., 2010, *Definition of the Floating System for Phase IV of OC3*, Technical Report NREL/TP-500-47535.

[12] Martin H.R., 2011, *Development of a Scale Model Wind Turbine for Testing of Offshore Floating Wind Turbine Systems*, M.S. Thesis, University of Maine, Orono.

[13] Rao S.S., 2004, *Mechanical Vibrations* 4th Ed., Pearson Prentice Hall, Upper Saddle River.

[14] The Norwegian Petroleum Directorate (NPD), 1992, *Guidelines Concerning Load Effects to Regulations Concerning Load Bearing Structures in the Petroleum Activities*.

[15] IEC 61400-3, 2009, *Wind Turbines - Part 3: Design Requirements for Offshore Wind Turbines*, International Electrotechnical Commission (IEC).

